



Supplement of

Spatiotemporal variability of CO₂, N₂O and CH₄ fluxes from a semi-deciduous tropical forest soil in the Congo Basin

Roxanne Daelman et al.

Correspondence to: Roxanne Daelman (roxanne.daelman@ugent.be)

The copyright of individual parts of the supplement might differ from the article licence.

Supplementary Material

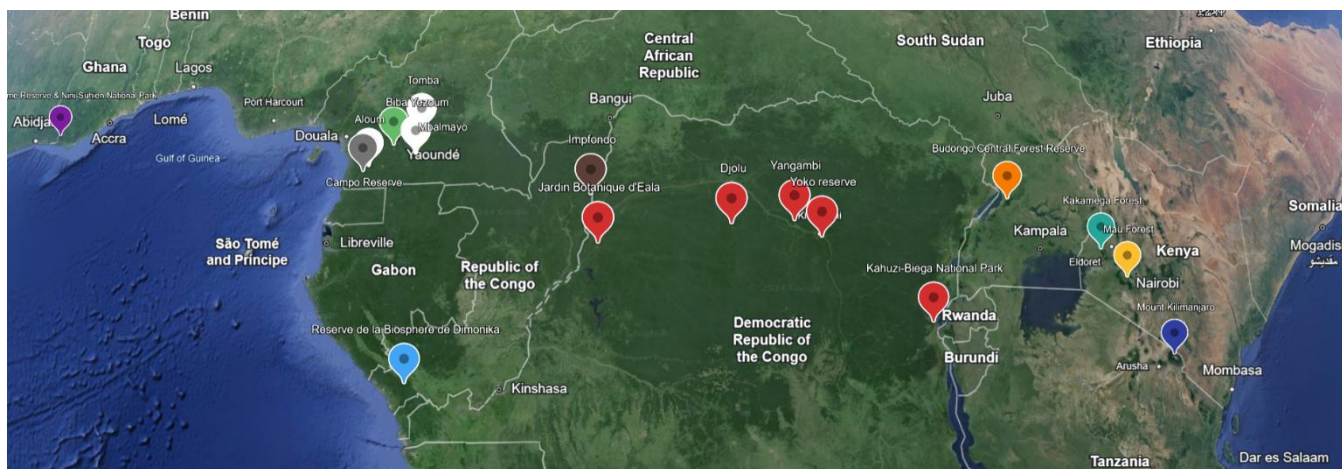


Figure S1: Different locations of studies which measured greenhouse gas fluxes of tropical forest soils in Central Africa. More information on the studies can be found in Table S1. Made using Google Earth 10.55.0.1 (Google, Landsat / Copernicus with data from SIO, NOAA, U.S. Navy, NGA, GEBCO, IBCAO) ©Google Earth

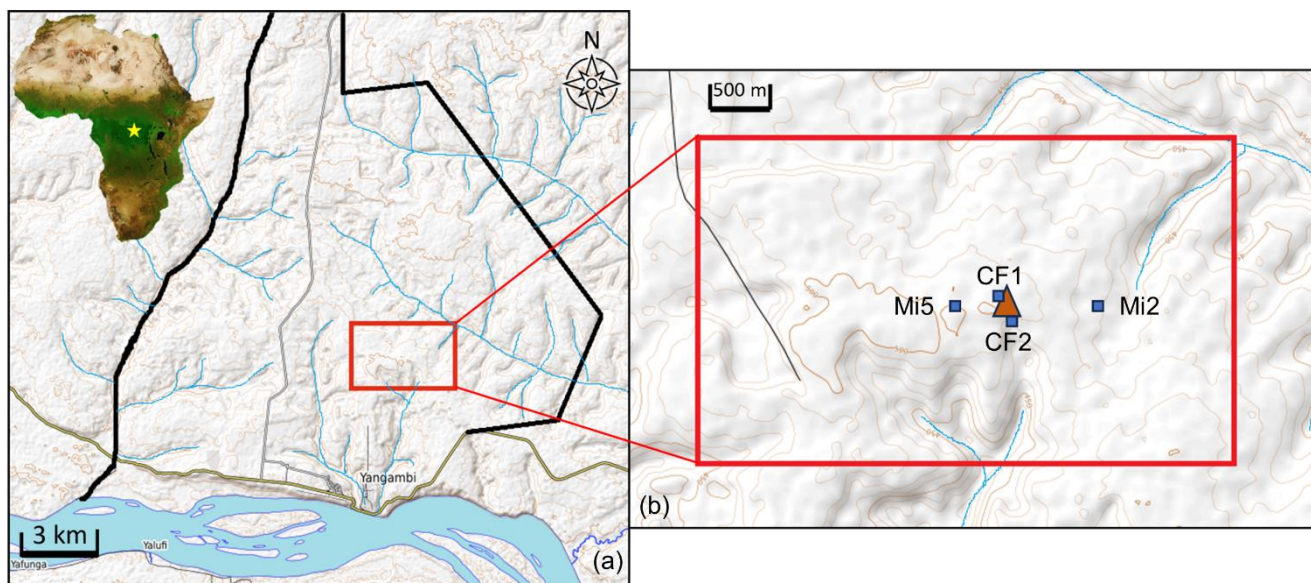


Figure S2: (a) Map of Yangambi with the CongoFlux climate site ($0^{\circ}48'52.0''$ N $24^{\circ}30'08.9''$ E) in the red square. (b) A close-up of the CongoFlux climate site with the triangle indicating the location of the flux tower and the squares indicating the locations of the 4 sampling plots (CF1, CF2, Mi2 and Mi5). Made using base map from OpenTopoMap.org (OpenStreetMap and SRTM)

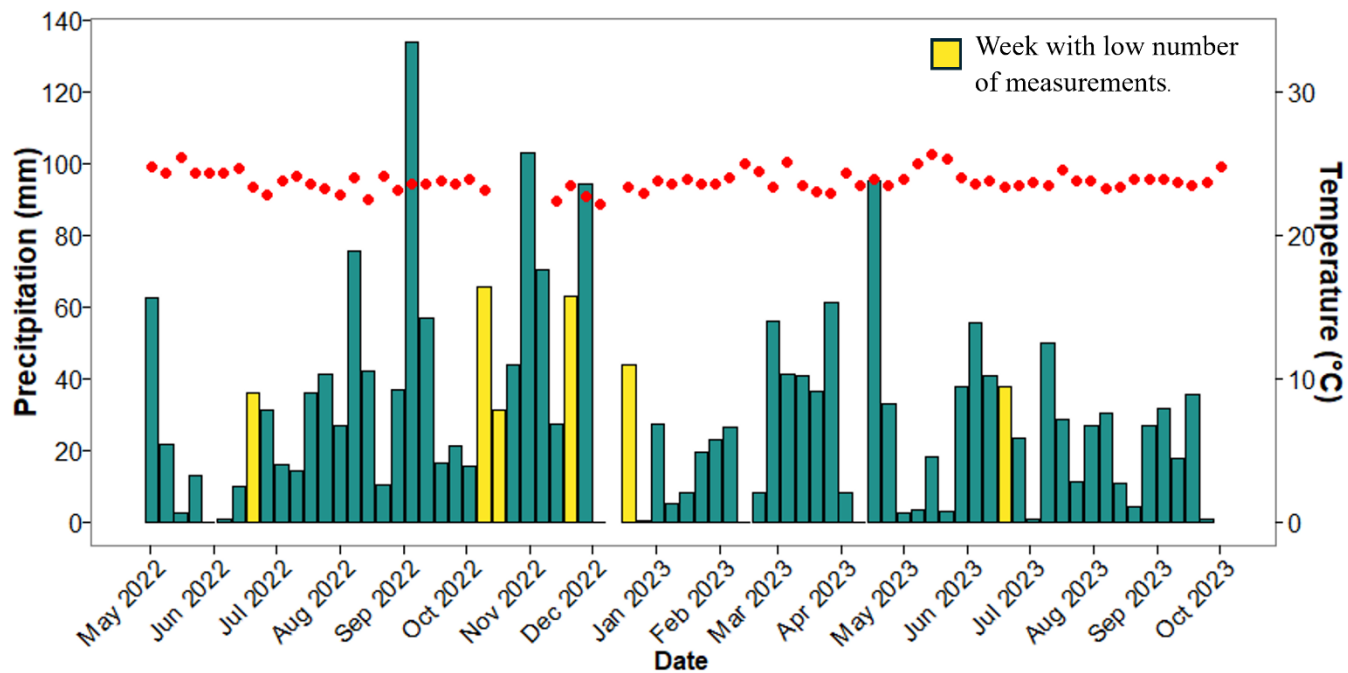


Figure S3: The bars showing the total precipitation (mm) per week and in red dotted line, the averaged air temperature per week (°C) at the CongoFlux site (0°48'52.0" N 24°30'08.9" E).

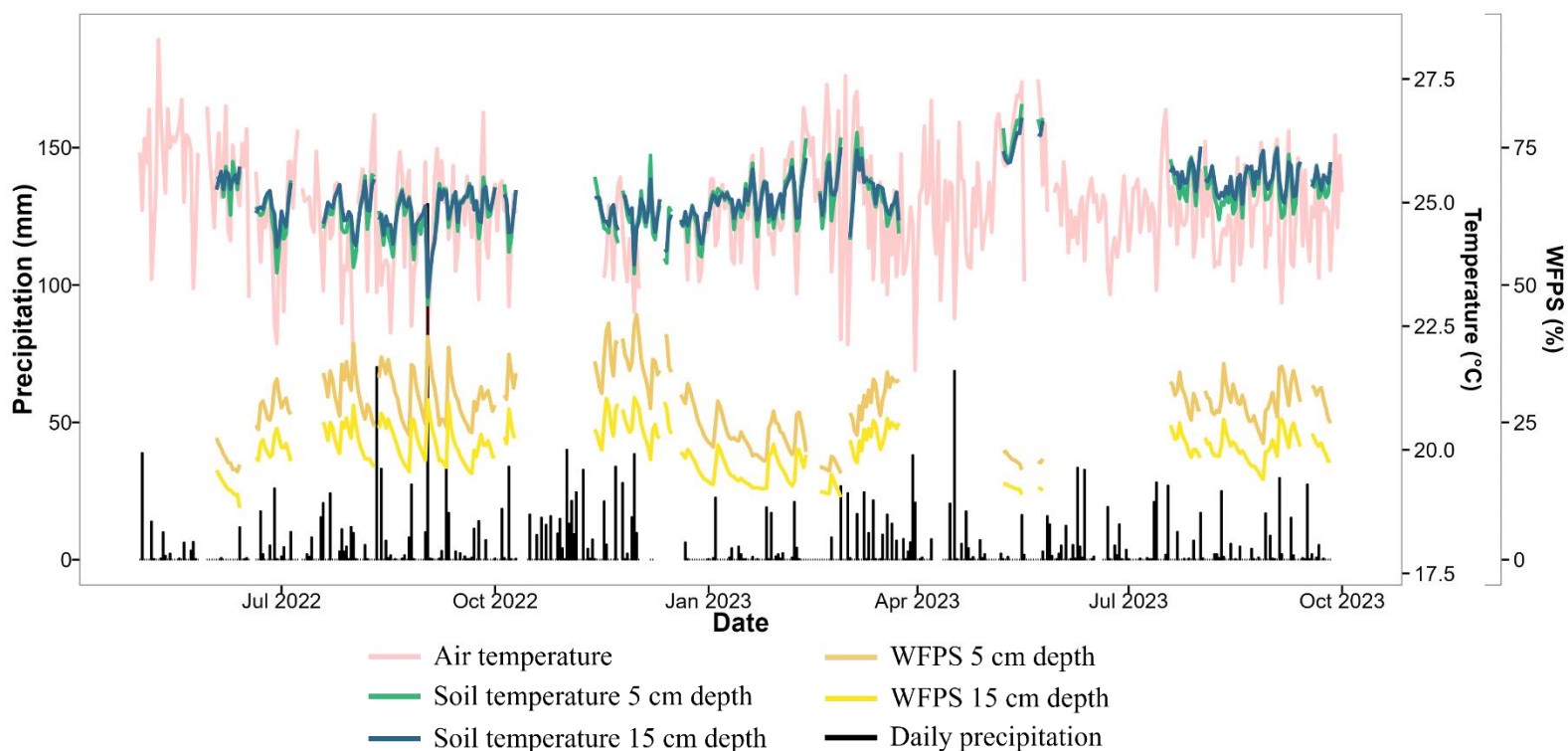


Figure S4: Water filled pore space (WFPS, %) and Soil Temperature (°C) daily average of the nine automated chamber locations at 5 cm and at 15 cm depth with daily precipitation (mm) and daily air temperature (°C) at the CongoFlux site (0°48'52.0" N 24°30'08.9" E).

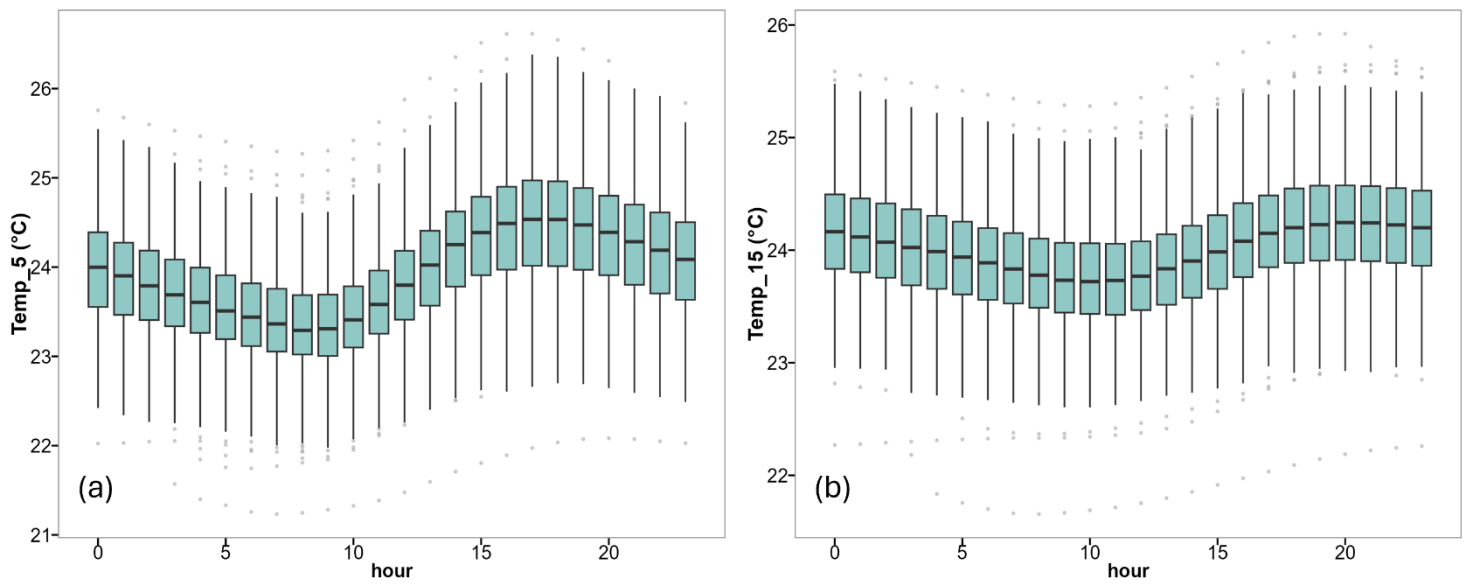


Figure S5: Diel cycle of the average of all nine automated chamber locations for a) soil temperature (Temp, °C) at 5 cm, and b) 15 cm depth . The boxplots show the median with the bold black line, the lower and upper hinges correspond to the 25th and 75th percentiles and the upper (lower) whisker extends from the hinge to the largest (smallest) value no further than 1.5 * inter-quartile range from the hinge. Data beyond the end of the whiskers are considered outlying points and are plotted individually. (June 1, 2022 – September 26, 2023, Yangambi, DRC)

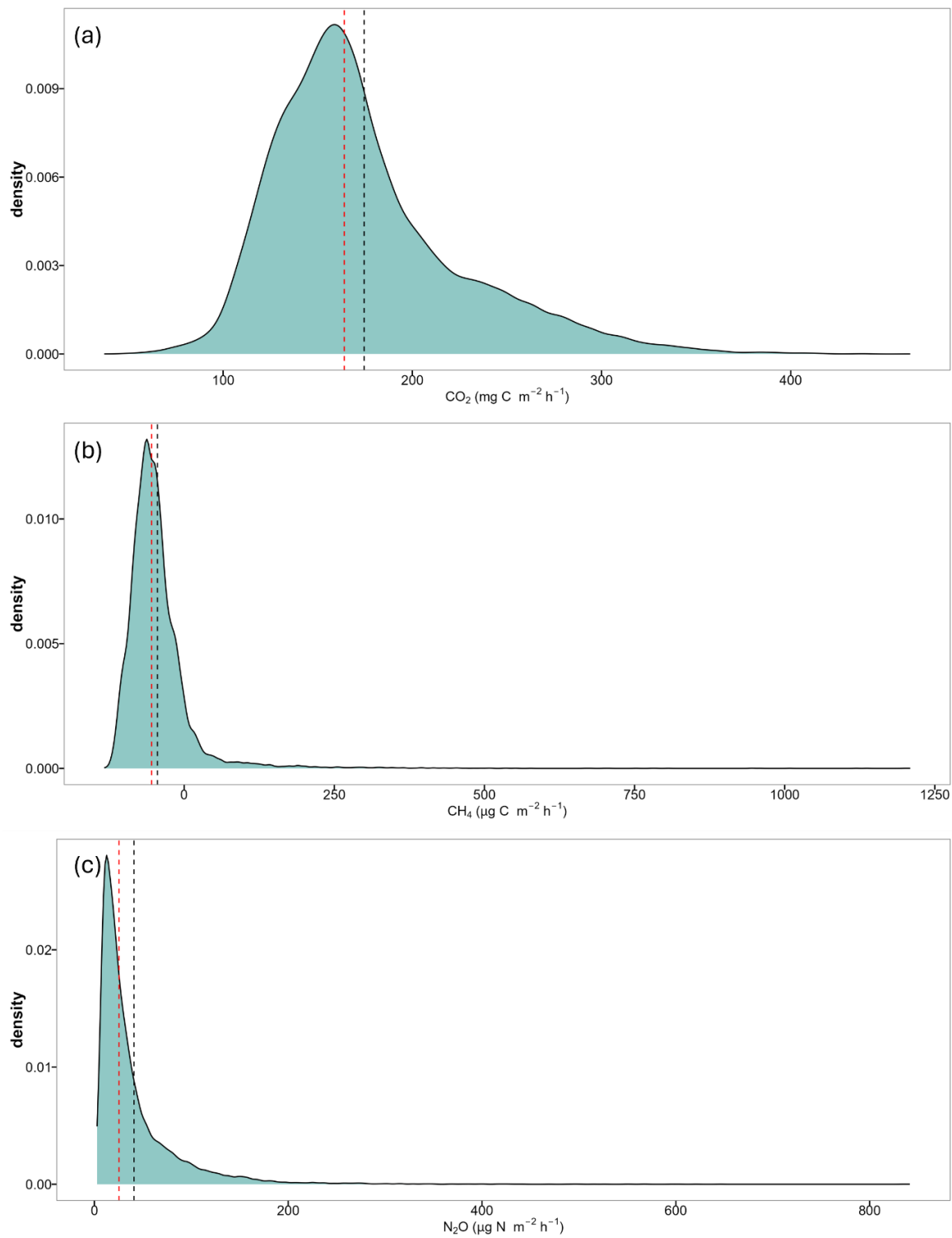


Figure S6: Distribution of all flux measurements during the whole measuring period (June 1, 2022 – September 26, 2023) of all nine automated chambers with the mean value in black and the median value in red dashed line for a) CO_2 (mg C m⁻² h⁻¹), b) CH_4 ($\mu\text{g C m}^{-2} \text{h}^{-1}$) and c) N_2O ($\mu\text{g N m}^{-2} \text{h}^{-1}$). (Yangambi, DRC)

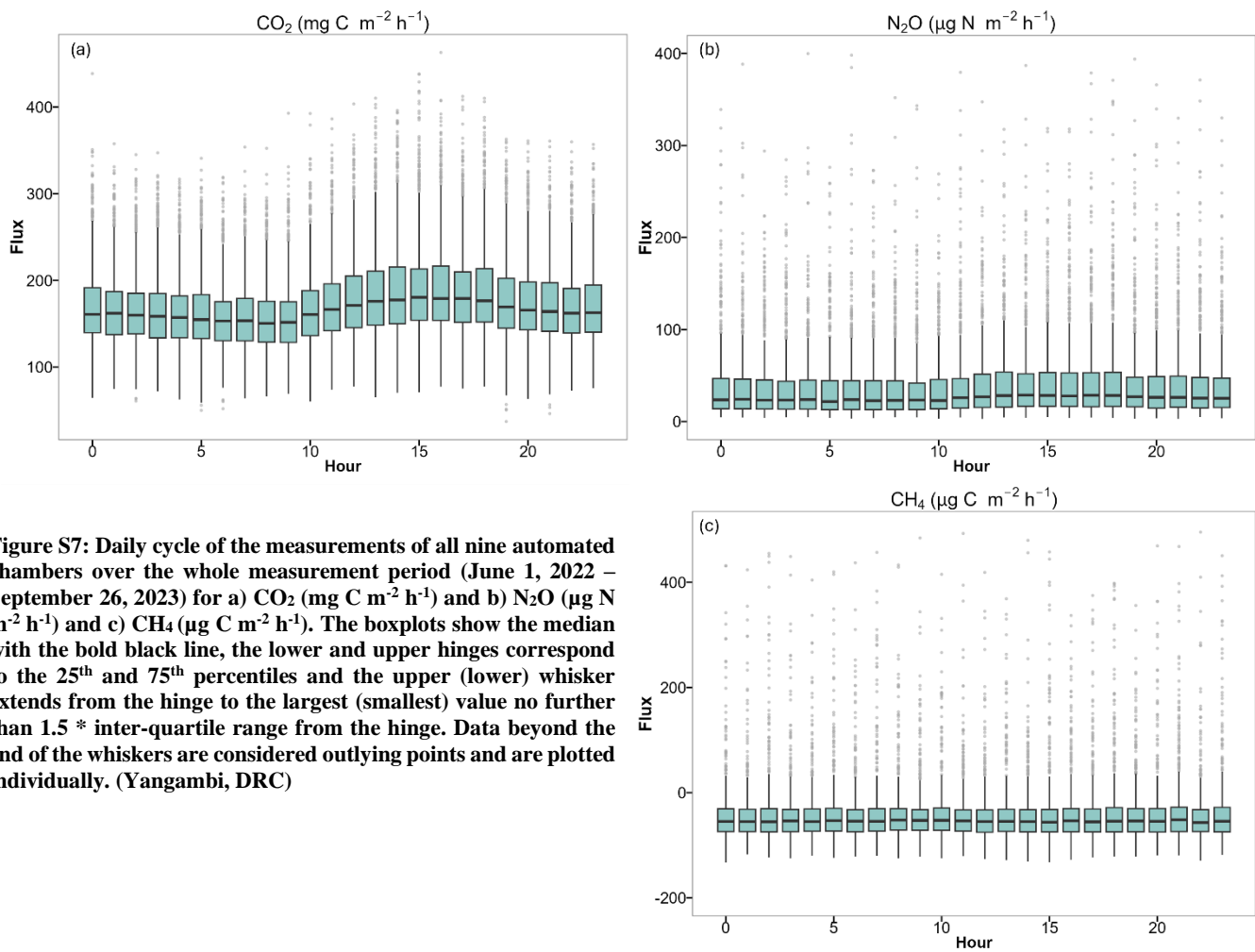


Figure S7: Daily cycle of the measurements of all nine automated chambers over the whole measurement period (June 1, 2022 – September 26, 2023) for a) CO₂ (mg C m⁻² h⁻¹) and b) N₂O (µg N m⁻² h⁻¹) and c) CH₄ (µg C m⁻² h⁻¹). The boxplots show the median with the bold black line, the lower and upper hinges correspond to the 25th and 75th percentiles and the upper (lower) whisker extends from the hinge to the largest (smallest) value no further than 1.5 * inter-quartile range from the hinge. Data beyond the end of the whiskers are considered outlying points and are plotted individually. (Yangambi, DRC)

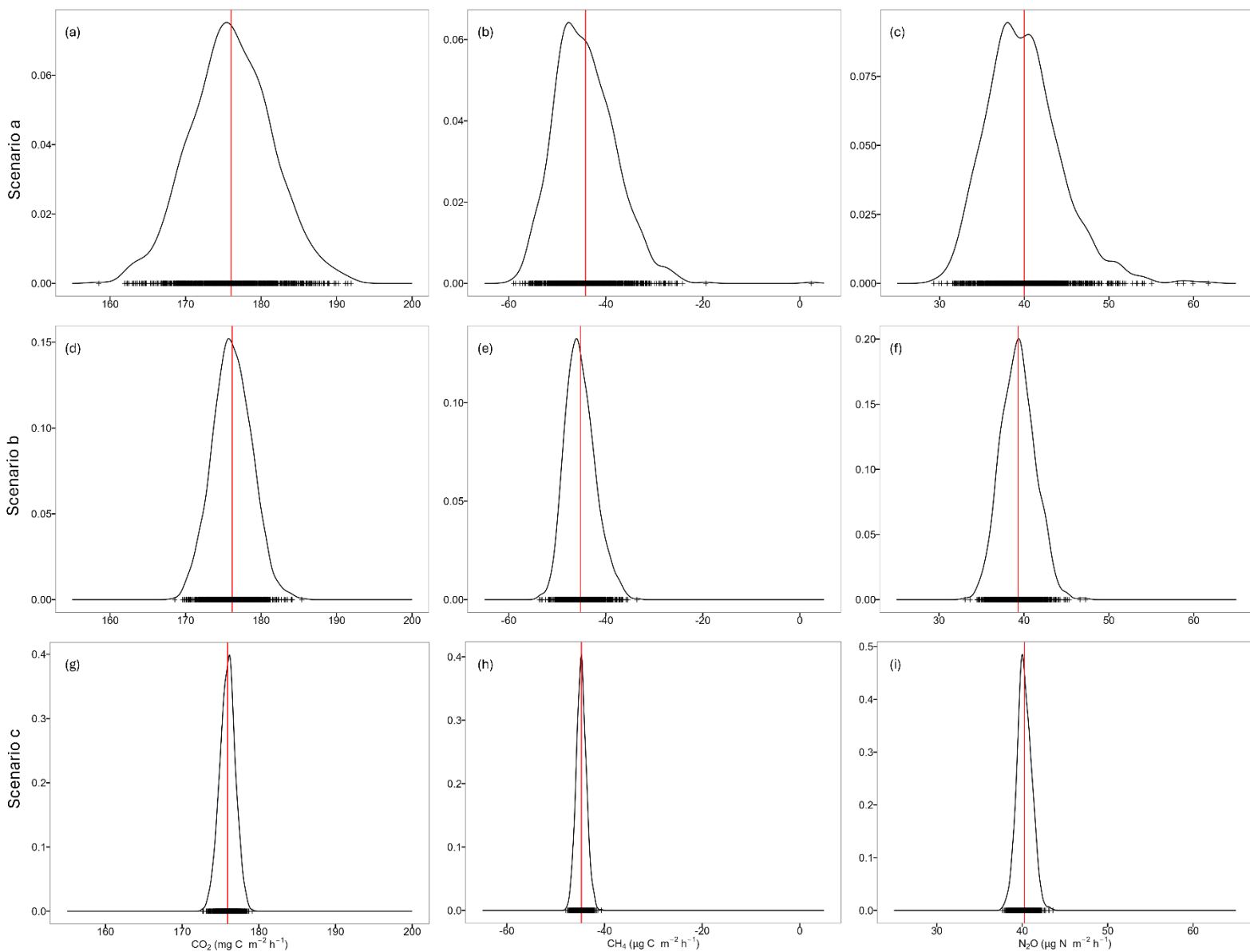


Figure S8: The distributions of the 1000 greenhouse gas budgets of the three bootstrap scenarios for the automated chamber measurements of CO₂ (g C m⁻² h⁻¹), CH₄ (mg C m⁻² h⁻¹) and N₂O (mg N m⁻² h⁻¹). More information about the resampling procedure can be found in Table S10.

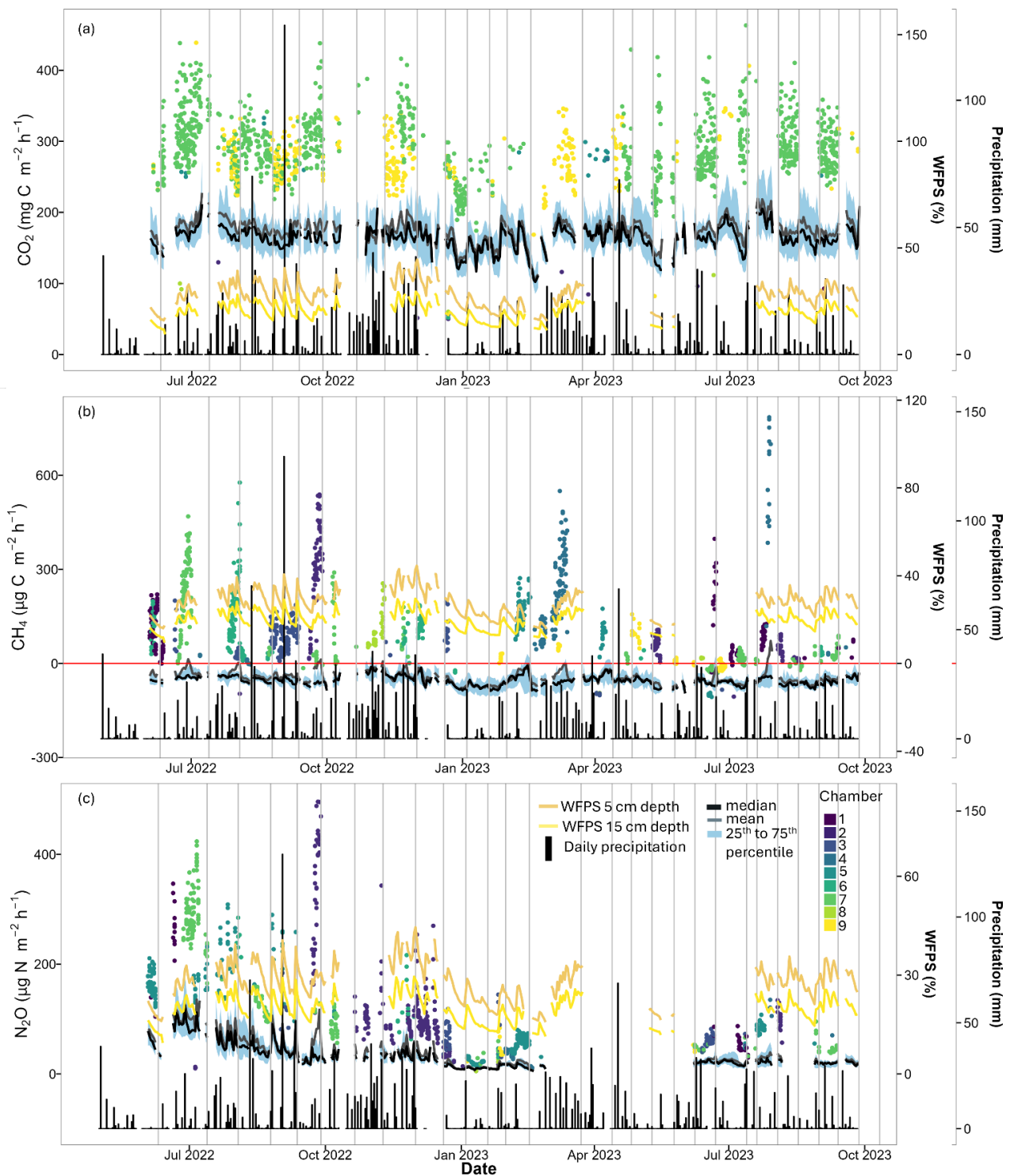


Figure S9: a) CO₂, b) CH₄ and c) N₂O fluxes of all nine automated chambers over the whole measuring period. In black are the daily median values, in grey the daily averages, in blue the 25th up to 75th quantile and the coloured points are outlier values. Outliers have a distance to the 25th or 75th quantile value that is larger than 1.5 times the interquartile distance. Each colour represents one chamber. Vertical grey lines depict days where the chambers were replaced from one collar to the other. Water filled pore space (WFPS, %) daily average of the nine automated chamber locations at 5 cm and at 15 cm depth with daily precipitation (mm). (Yangambi, DRC)

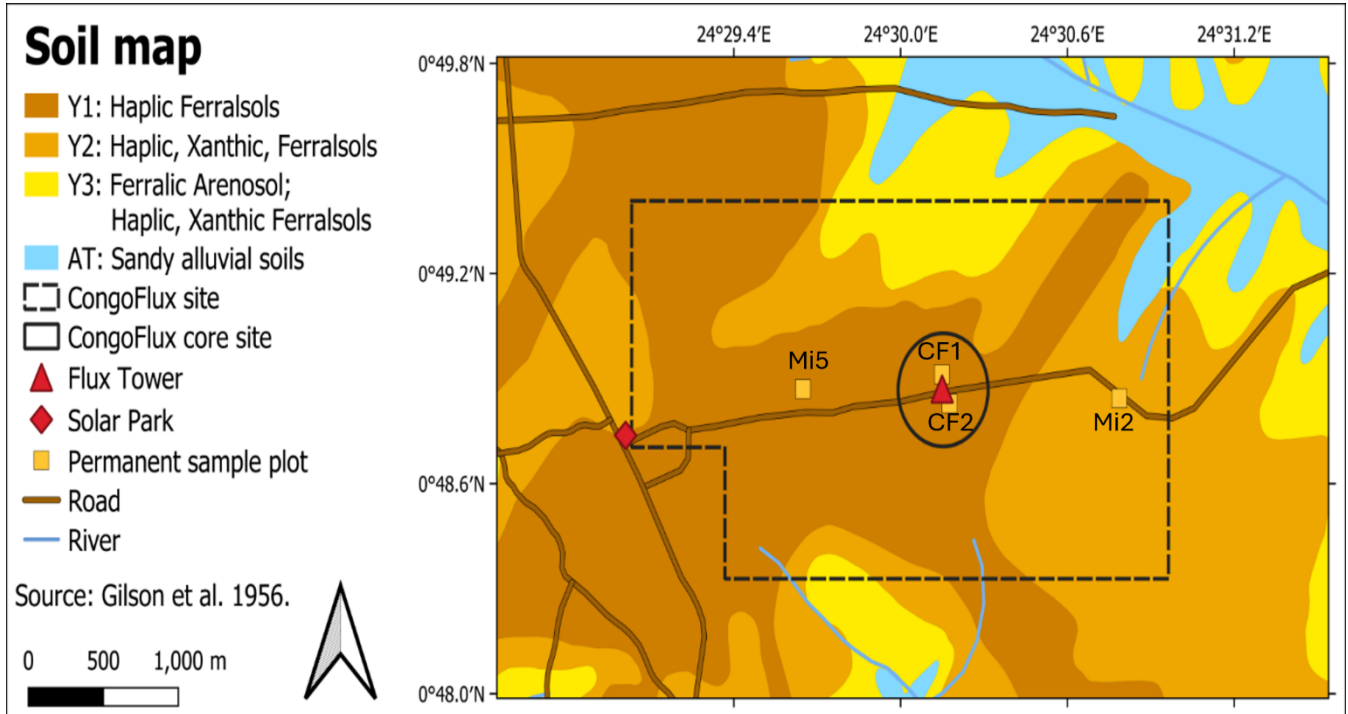


Figure S10: Soil map of Yangambi with the CongoFlux climate site (0°48'52.0" N 24°30'08.9" E) in the black dotted line tower and the squares indicating the locations of the 4 sampling plots (CF1, CF2, Mi2 and Mi5). Source for the map is: Gibson et al., 1956.

To evaluate the two methods used in this study, i.e. fast box and automated chamber method, a comparison between the measurements of the automated chambers and the measurements of the fast box chambers closest located to the automated chambers (plot CF1) was made during the overlapping time period. The fast box measurements from the CF1 plot for CO₂ were quite comparable with those of the automated chambers over the same time period (S11 a). The spread for the fast box method was larger, which was to be expected since there were more locations of the fast box chambers and the chambers were smaller in size. In both the automated and the fast box measurements, positive fluxes for CH₄ were present, but they were dominated by negative fluxes (S11 b). Especially in the second half of August the fast box fluxes tended to be more negative than the fluxes of the automated chambers. For N₂O no real comparison could be made due to the malfunction of the N₂O analyser of the automated soil chamber set-up. Therefore, the measurements of July and September from the automated chambers were compared to the measurements of August of the fast box chambers (S11 c). Our results showed that the fast box measurements were generally higher than the automated measurements. The mismatch of dates could lead to a discrepancy in the averages, especially because we saw a slight increase in flux for some automated chambers in early August and then a decrease again at the end of August, which could indicate a period of higher fluxes that is missed here. This discrepancy could also be due to altered soil conditions at the automated chamber locations due to the long-term deployment on the same location, however no clear differences for the other GHG were detected in this period and the location of the chambers was consistently changed between to collars, so this effect should be minor.

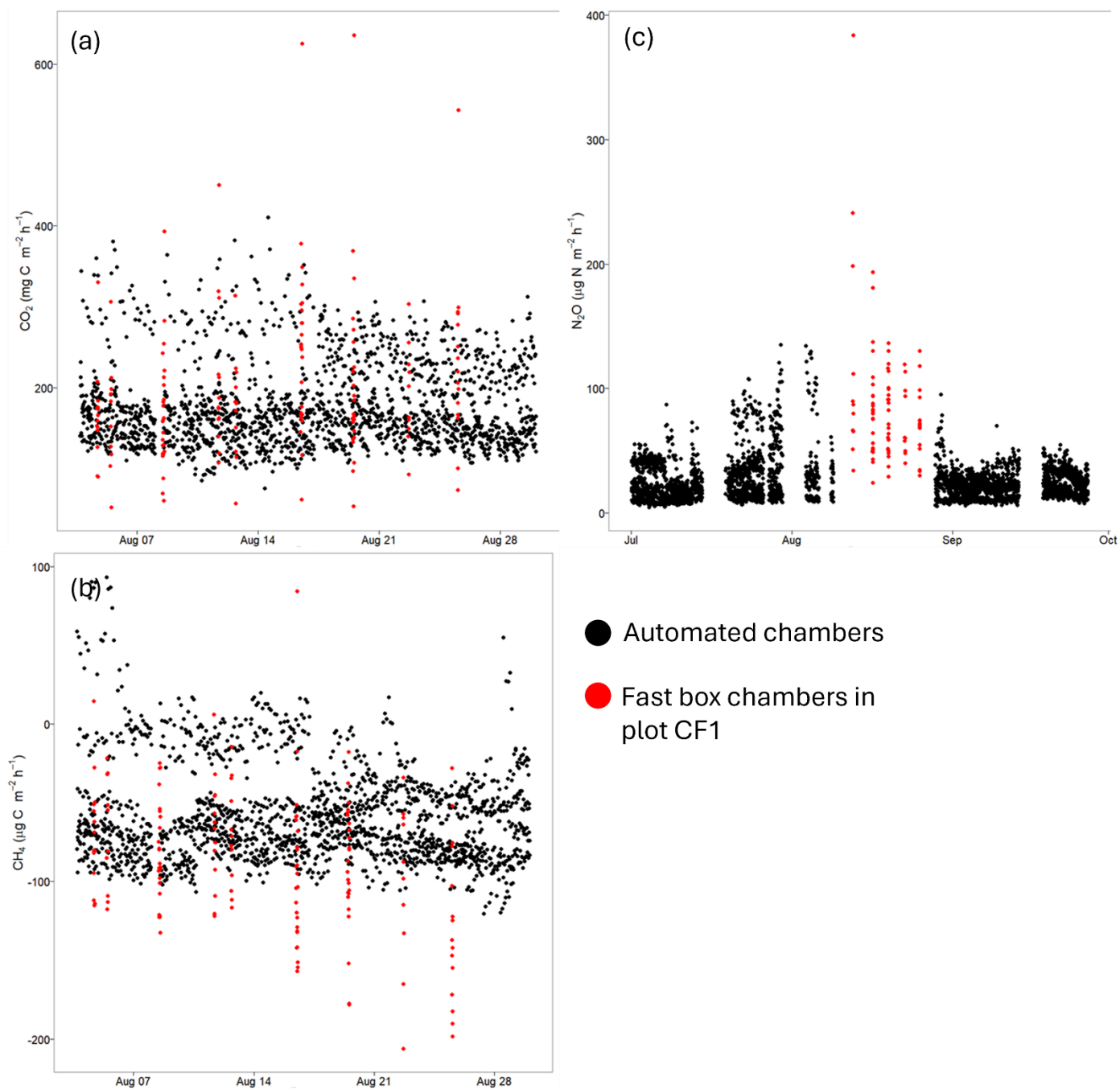









Figure S11: Flux measurements for a) CO₂, b) CH₄ and c) N₂O, with in red the measurements from the fast box chambers in plot CF1 and in black the measurements from all automated chambers.

Table S1: Different studies which measured greenhouse gas fluxes of tropical forest soils in sub-Saharan Africa. Locations of the studies can be found on the map in Fig. S1.

Country	Location	Research team	Method	Focus
Kenya	 Mau Forest Complex	Arias-Navarro et al. 2017a	Soil laboratory incubations for N ₂ O	Topography
		Arias-Navarro et al. 2017b	Soil laboratory incubations for N ₂ O and CO ₂	Land use
		Wanyama et al. 2018	Manual static chamber for N ₂ O	Management intensity
		Wanyama et al. 2019	Manual static chamber for CO ₂ and CH ₄	Land use
	 Kakamega Forest National Park	Werner et al. 2007	Automated static chamber for CO ₂ , CH ₄ and N ₂ O	Tropical Forest
DRC	 Maringa Lopori-Wamba Landscape, Yangambi Biosphere Reserve, Yoko Forest Reserve, Jardin Botanique d'Eala, Kahuzi-Biéga National Park	Barthel et al. 2022	Manual static chamber for CH ₄ and N ₂ O	Montane, swamp and lowland forest
		Baumgartner et al. 2020	Manual static chamber for CO ₂	Montane and lowland forest
Ghana	 Ankasa Wildlife Protected Area	Castaldi et al. 2013	Manual static chamber for N ₂ O	Tropical forest
		Castaldi et al. 2020	Manual static chamber for CH ₄	Tropical forest
Tanzania	 Mount Kilimanjaro	Gütlein et al. 2018	Soil laboratory incubations and manual static chamber for CO ₂ , CH ₄ and N ₂ O	Different ecosystems
Cameroon	 Aloum, Biba Yezoum, Tomba	Iddris et al. 2020	Manual static chamber for N ₂ O	Rain forest and Cacao agroforest
	 Campo-Ma'an	Tchiofo Lontsi et al. 2020	Manual static chamber for CO ₂ , CH ₄ and N ₂ O	Tropical forest





	 Mbalmayo Forest Reserve	Macdonald et al. 1998	Manual static chamber for CH ₄	Termite mounds
Republic of Congo	 Dimonika Natural Park Forest	Serca et al. 1994	Manual static chamber for N ₂ O	Tropical forest
	 Impfondo	Tathy et al. 1992	Manual static chamber for CO ₂ and CH ₄	Flooded forest
Uganda	 Budongo Central Forest Reserve	Tamale et al. 2021	Manual static chamber for CO ₂ , CH ₄ and N ₂ O	Nutrient limitation

Table S2: The concentration of exchangeable basic cations calcium (Ca), potassium (K), magnesium (Mg) and Sodium (Na) and the cation exchange capacity (CEC), expressed as centimoles per kilogram of dry soil (cmol(+) kg⁻¹), the pH values measured both in water (pH w) and in kaliumchloride (pH KCl), the nitrogen (N) and carbon (C) content expressed as percentages, the phosphorus (P) concentration expressed in ppm and the weight percentage of sand, soil and clay for each different soil layer at specific depths expressed in centimetres. This analysis was carried out in the CF1 plot at the CongoFlux site (0°48'52.0" N 24°30'08.9" E).

		Exchangeable basic cations and CEC								
Horizon	Depth	Ca	K	Mg	Na	CEC				
Ah1	0-8/12	0.22	0.10	0.14	0.01	7.10				
Ah2	8/12-19/38	0.34	0.02	0.04	0.01	3.80				
AB	38-62	0.26	< 0.01	0.02	< 0.01	4.10				
Bws1	62-110	0.29	0.01	0.01	< 0.01	3.30				
Bws2	110-136	0.52	< 0.01	0.01	< 0.01	3.10				
Bws3	136-160+	0.21	< 0.01	< 0.01	< 0.01	2.60				
		pH					Soil texture			
Horizon	Depth	pH w	pH KCl	N	C	P	Sand	Silt	Clay	
Ah1	0-8/12	3.73	3.52	0.15	2.09	7.09	66.54	2.49	30.97	
Ah2	8/12-19/38	4.26	3.82	0.28	0.58	4.75	69.29	0.98	29.73	
AB	38-62	4.41	3.85	0.21	0.45	3.95	62.64	1.25	36.11	
Bws1	62-110	4.43	3.89	0.17	0.34	3.97	58.39	1.86	39.75	
Bws2	110-136	4.41	3.84	0.13	0.26	2.41	59.16	1.89	38.96	
Bws3	136-160+	4.32	3.88	0.11	1.12	2.53	60.86	0.62	38.52	

Table S3: Monthly accumulated rainfall from half hourly measurements with the amount of missing datapoints, monthly averaged air temperature (Temp) from hourly measurements, with the amount of missing datapoints, monthly averaged water filled pore space (WFPS) and monthly averaged soil temperature from hourly measurements, on 5 cm and 15 cm depth with the amount of missing data points, measured at the CongoFlux site (0°48'52.0" N 24°30'08.9" E).

Month	Rainfall (mm)	NA 30'	Temp (°C)	NA 60'	WFPS_5 (%)	WFPS_15 (%)	Temp_5 (°C)	Temp_15 (°C)	NA 60'
June 2022	69.40	187	23.83	93	22.87	16.91	23.94	24.05	99
July 2022	127.31	74	23.58	36	30.67	22.22	23.70	23.84	261
August 2022	167.67	19	23.33	52	30.32	21.60	23.53	23.64	0
September 2022	237.91	45	23.65	7	29.03	20.41	23.72	23.75	0
October 2022	176.73	291	23.60	518	31.16	22.21	23.58	23.68	449
November 2022	325.63	145	23.13	422	36.88	25.00	23.58	23.66	362
December 2022	41.43	912	23.09	479	31.42	20.76	23.45	23.53	81
January 2023	76.03	0	23.64	0	22.47	15.81	23.86	23.90	23
February 2023	64.39	9	24.29	4	20.27	14.99	24.16	24.16	196
March 2023	205.25	54	23.58	23	29.13	22.41	24.03	24.09	192
April 2023	163.20	251	23.75	0	/	/	/	/	720
May 2023	54.65	0	24.91	202	18.57	13.48	25.20	25.06	492
June 2023	162.20	257	23.57	43	/	/	/	/	720
July 2023	98.14	17	23.85	1	29.79	21.46	24.32	24.46	440
August 2023	90.93	30	23.62	32	27.85	19.48	24.17	24.32	28
September 2023	103.03	0	23.75	7	30.41	21.71	24.23	24.38	0

Table S4: Monthly accumulated soil CO₂ (g C m⁻²), CH₄ (mg C m⁻²) and N₂O (mg N m⁻²) exchange from all nine automated chambers. Days with no measurement were linearly interpolated if the gap was smaller than 10 consecutive days, otherwise the gap was not filled. All gaps in the CO₂ and CH₄ measurements were filled. An accumulated year budget for all three greenhouse gasses (CO₂ in Mg C ha⁻¹, CH₄ in kg C ha⁻¹ and N₂O in kg N ha⁻¹) is calculated for all 12 consecutive months. (Yangambi, DRC)

Month	CO ₂ (g C m ⁻²)	CH ₄ (mg C m ⁻²)	Gap filled	N ₂ O (mg N m ⁻²)	Gap filled	NA
June 2022	114.3	-21.0	8	53.7	8	0
July 2022	147.7	-25.1	8	66.6	8	0
August 2022	131.3	-30.2	1	44.7	1	0
September 2022	128.3	-27.7	2	33.7	1	0
October 2022	133.8	-24.9	17	30.2	18	0
November 2022	129.5	-21.0	2	30.8	8	0
December 2022	121.0	-35.4	4	22.1	4	0
January 2023	116.8	-52.4	0	8.9	0	0
February 2023	100.6	-29.0	2	10.5	3	1
March 2023	130.9	-28.3	7	/	0	31
April 2023	129.2	-30.5	0	/	0	30
May 2023	117.5	-48.4	8	/	0	31
June 2023	128.1	-39.4	5	14.0	0	6
July 2023	141.9	-30.5	5	19.0	5	0
August 2023	131.3	-41.5	2	8.1	3	19
September 2023	116.4	-28.5	4	14.3	4	0
Year	(Mg C ha ⁻¹)	(kg C ha ⁻¹)		(kg N ha ⁻¹)		
June 2022-May 2023	15.0	-3.7	59	3.0	51	93
July 2022-June 2023	15.1	-3.9	56	2.6	43	99
August 2022-July 2023	15.1	-4.0	53	2.1	40	99
September 2022-August 2023	15.1	-4.1	54	1.8	42	118
October 2022-September 2023	15.0	-4.1	56	1.6	45	118

Table S5: The average of the daily means (337 days) of water filled pore space (WFPS, %) and temperature (Temp, °C) at 5 cm and 15 cm depth per sensor (*mean* ^{*max*}/_{*min*}). Different letters point to statistical difference based on the Kruskal-Wallice test followed by the Wilcox test (Bonferroni adjusted p-value <0.05) measured at the CongoFlux site (0°48'52.0" N 24°30'08.9" E), (June 1, 2022 – September 26, 2023).

	1	2	3	4	5	6	7	8	9
WFPS_5	23.1 ^{38.8} _{14.8}	32.2 ^{47.1} _{16.4}	29.0 ^{46.1} _{19.0}	20.6 ^{34.6} _{11.3}	21.6 ^{36.3} _{12.6}	24.1 ^{39.8} _{13.9}	22.7 ^{39.2} _{14.2}	34.3 ^{54.3} _{14.7}	43.7 ^{69.1} _{18.0}
	AB	C	D	E	EF	A	BF	G	H
WFPS_15	12.3 ^{23.6} _{7.0}	23.3 ^{34.0} _{13.5}	22.9 ^{33.4} _{14.9}	22.2 ^{33.5} _{13.8}	14.6 ^{24.4} _{7.23}	27.9 ^{41.9} _{18.9}	11.6 ^{21.6} _{6.5}	18.3 ^{28.3} _{9.8}	25.6 ^{42.0} _{12.1}
	A	B	BC	C	D	E	A	F	G
Temp_5	23.9 ^{25.8} _{21.9}	23.6 ^{25.8} _{21.9}	23.9 ^{25.8} _{21.7}	24.0 ^{25.8} _{22.0}	24.0 ^{25.7} _{21.9}	23.9 ^{25.9} _{21.9}	24.1 ^{26.1} _{21.9}	23.8 ^{25.8} _{21.7}	24.2 ^{26.0} _{21.9}
	AB	C	ADE	DFG	AF	ABG	F	BE	/
Temp_15	23.9 ^{25.7} _{22.1}	23.2 ^{25.6} _{22.2}	23.9 ^{25.4} _{22.0}	24.0 ^{25.5} _{22.2}	24.0 ^{25.7} _{21.9}	24.0 ^{25.5} _{22.3}	24.2 ^{25.6} _{22.3}	23.8 ^{25.5} _{21.9}	24.4 ^{25.9} _{21.3}
	A	B	A	A	A	A	C	B	D

Table S6: Soil CO₂ (mg C m⁻² h⁻¹), CH₄ (μg C m⁻² h⁻¹) and N₂O (μg N m⁻² h⁻¹) exchange during the whole measurement period (June 1, 2022 – September 26, 2023) for each automated chamber separately showing the mean with standard deviation (*mean* ± *SD*) followed by the coefficient of variation (CV) and the median with the minimum and maximum value (*median*_{min}^{max}). The last row ‘All chambers’ indicates the average of the 9 mean values together with its standard deviation and CV. The first column indicates the chamber number, the fourth column indicates the amount of CO₂ and CH₄ data points and the sixth column indicates the amount of N₂O data points. (Yangambi, DRC)

Chamber	CO ₂	CH ₄	#meas	N ₂ O	#meas
Collar	(mg C m ⁻² h ⁻¹)	(μg C m ⁻² h ⁻¹)		(μg N m ⁻² h ⁻¹)	
Chamber 1	151.8 ± 20.0	-49.5 ± 56.9	1048	32.8 ± 25.4	655
1	CV: 0.13 150.2 ₉₁ ²⁶²	CV: 1.15 -60.33 ₋₁₀₆ ³⁹⁸		CV: 0.78 26.2 ₆ ¹⁴³	
2	167.2 ± 23.2 CV: 0.14 166.9 ₇₃ ²⁴⁶	-45.7 ± 39.0 CV: 0.85 -56.2 ₋₁₀₂ ²⁵³	1206	48.0 ± 58.3 CV: 1.21 23.4 ₇ ³⁴⁷	823
Chamber 2	140.9 ± 24.6	-63.6 ± 38.8	1327	28.8 ± 27.1	991
1	CV: 0.17 137.9 ₅₀ ²³²	CV: 0.61 -72.9 ₋₁₃₁ ¹⁰⁷		CV: 0.94 17.1 ₆ ¹⁶³	
2	134.2 ± 24.9 CV: 0.19 134.8 ₃₇ ²⁰⁴	-35.0 ± 84.4 CV: 2.41 -47.7 ₋₁₂₀ ⁵³⁹	1497	41.7 ± 87.9 CV: 2.11 14.6 ₇ ⁸⁴²	1233
Chamber 3	149.0 ± 24.3	-52.5 ± 55.1	1519	39.2 ± 29.1	1077
1	CV: 0.16 153.3 ₅₆ ²³¹	CV: 1.05 -69.1 ₋₁₂₉ ¹⁹⁷		CV: 0.74 31.0 ₃ ¹⁸⁴	
2	158.5 ± 23.6 CV: 0.15 158.5 ₅₇ ²⁹⁴	-80.5 ± 27.2 CV: 0.34 -81.1 ₋₁₂₆ ²⁰⁰	1535	38.3 ± 33.8 CV: 0.88 28.3 ₃ ²²⁷	1164

Chamber 4	170.2 ± 26.0	-24.6 ± 81.1	1397	32.6 ± 24.8	1046
1	CV: 0.15 168.3^{277}_{68}	CV: 3.30 -44.5^{550}_{-103}		CV: 0.76 22.9^{141}_4	
2	186.5 ± 26.3 CV: 0.14 184.8^{302}_{65}	-19.8 ± 108.3 CV: 5.51 -34.2^{1209}_{-102}	1424	38.9 ± 31.8 CV: 0.82 29.0^{216}_6	1108
Chamber 5	169.9 ± 26.8	-85.0 ± 20.0	1519	54.6 ± 63.0	1076
1	CV: 0.16 168.6^{291}_{61}	CV: 0.23 -88.1^{-32}_{-133}		CV: 1.15 22.7^{309}_5	
2	211.9 ± 29.1 CV: 0.14 211.4^{333}_{81}	-51.3 ± 59.2 CV: 1.15 -65.2^{272}_{-132}	1627	63.4 ± 44.7 CV: 0.71 44.9^{235}_9	1216
Chamber 6	154.7 ± 23.3	-20.5 ± 49.8	2765	36.7 ± 39.0	1969
	CV: 0.15 154.6^{254}_{52}	CV: 2.43 -29.3^{577}_{-84}		CV: 1.06 17.1^{284}_3	
Chamber 7	263.1 ± 44.5	-19.2 ± 39.1	1155	50.1 ± 40.3	935
1	CV: 0.17 259.3^{429}_{105}	CV: 2.04 -27.1^{290}_{-74}		CV: 0.81 37.0^{228}_5	
2	261.5 ± 50.5 CV: 0.19 $258.2^{463}_{91.6}$	-11.8 ± 70.5 CV: 5.98 -29.5^{469}_{-81}	1329	65.4 ± 81.9 CV: 1.25 25.0^{424}_7	1103

Chamber 8	132.4 ± 19.5	-64.4 ± 16.7	1368	25.4 ± 17.6	942
1	CV: 0.15 $133.4 \frac{232}{60}$	CV: 0.26 $-65.0 \frac{19}{-106}$		CV: 0.69 $20.6 \frac{127}{5}$	
2	124.4 ± 15.6 CV: 0.13 $123.8 \frac{220}{53}$	-62.8 ± 38.0 CV: 0.61 $-68.2 \frac{255}{-120}$	1572	22.9 ± 16.1 CV: 0.70 $18.9 \frac{85}{3}$	1165
Chamber 9	224.0 ± 49.0	-40.6 ± 24.4	1351	36.0 ± 22.1	969
1	CV: 0.22 $232.1 \frac{406}{76}$	CV: 0.60 $-43.1 \frac{62}{-100}$		CV: 0.61 $27.8 \frac{131}{5}$	
2	201.1 ± 47.1 CV: 0.23 $186.1 \frac{439}{46}$	-41.5 ± 32.7 CV: 0.79 $-48.0 \frac{157}{-98}$	1570	37.8 ± 21.0 CV: 0.56 $33.9 \frac{148}{6}$	1163
All chambers	176.6 ± 42.6 CV: 0.24	-45.2 ± 21.8 CV: 0.48	/	40.7 ± 12.1 CV: 0.30	/

Table S7: The linear mixed effect model fitted on the CO₂ fluxes (mg C m⁻² h⁻¹) from the automated chambers followed by the fixed effects of water filled pore space (WFPS, %), soil temperature (Temp_{soil}, °C), air temperature (Temp_{air}, °C), precipitation (Rain, mm) and the accumulated precipitation in the previous 10 days (PrevRain_{10days}, mm) in absolute value (not relative change), the t-values, the partial R² (%) and the variance of inflation factor (VIF) of the fixed factors and the conditional and marginal R² (%) of the model. The chamber number with collar is used as random intercept and an autoregressive model of order one is included to account for the temporal correlation in the data (CorAR1).

$$\log(Flux_{CO_2}) \sim WFPS + Temp_{soil} + Temp_{air} + Rain + PrevRain_{10days} + (1|ChamberID) + CorAR1$$

	Fixed effect size	t-value	Partial R ²	VIF
WFPS	0.0084	25.5	0.05	1.5
Temp _{soil}	0.0681	36.1	0.07	1.2
Temp _{air}	0.0184	46.6	0.04	1.0
Rain	0.0059	7.6	0.01	1.0
PrevRain _{10days}	0.0009	12.5	0	1.3
Conditional R ²	0.79			
Marginal R ²	0.13			

Table S8: The linear mixed effect model fitted on the CH₄ fluxes (µg C m⁻² h⁻¹) from the automated chambers followed by the fixed effects of water filled pore space (WFPS, %), air temperature (Temp_{air}, °C) and the accumulated precipitation in the previous 10 days (PrevRain_{10days}, mm) in absolute value (not relative change), the t-values and the partial R² and the variance of inflation factor (VIF) of the fixed factors and the conditional and marginal R² of the model. The chamber number with collar is used as random intercept and an autoregressive model of order one is included to account for the temporal correlation in the data (CorAR1).

$$\log(Flux_{CH_4} + min) \sim WFPS + Temp_{air} + PrevRain_{10days} + (1|ChamberID) + CorAR1$$

	Fixed effect size	t-value	Partial R ²	VIF
WFPS	0.0061	11.4	0.02	1.2
Temp _{air}	-0.0045	-8.0	0.01	1.0
PrevRain _{10days}	0.0022	13.1	0.02	1.3
Conditional R ²	0.35			
Marginal R ²	0.05			

Table S9: The linear mixed effect model fitted on the N₂O (µg N m⁻² h⁻¹) fluxes from the automated chambers followed by the fixed effects of water filled pore space (WFPS, %), soil temperature (Temp_{soil}, °C), air temperature (Temp_{air}, °C) and the accumulated precipitation in the previous 10 days (PrevRain_{10days}, mm) in absolute value (not relative change), the t-values and the partial R² and the variance of inflation factor (VIF) of the fixed factors and the conditional and marginal R² of the model. The chamber number with collar is used as random intercept and an autoregressive model of order one is included to account for the temporal correlation in the data (CorAR1).

$$\log(Flux_{N_2O}) \sim WFPS + Temp_{soil} + Temp_{air} + PrevRain_{10days} + (1|ChamberID) + CorAR1$$

	Fixed effect size	t-value	Partial R ²	VIF
WFPS	0.0285	37.5	0.05	1.4
Temp _{soil}	0.0895	22.9	0.02	1.1
Temp _{air}	0.0193	25.9	0.01	1.0
PrevRain _{10days}	0.0034	16.0	0.01	1.3
Conditional R ²	0.22			
Marginal R ²	0.12			

To look into the effect of the high sampling frequency of the set-up, a resampling procedure was carried out to simulate lower sampling frequencies with the same number of chambers. For this resampling only daytime measurements were used. The resampling scenarios were **a**) one measurement per chamber every month, **b**) one measurement per chamber every week, and **c**) one measurement per chamber every day. Using a bootstrapping procedure (size 1000), one measurement per chamber is randomly selected out of the subset per period (month, week or day) of the data of the whole measurement period. The mean of the nine chambers was calculated per period (month, week or day) and then the average of all periods was taken as GHG budget. The budget of scenario **a** is the average of 16 measurements per chamber, scenario **b** has 69 measurements per chamber for CO₂ and CH₄ and 56 for N₂O and scenario **c** has 380 measurements per chamber for CO₂ and CH₄ and 270 for N₂O. In Table S10, the mean together with the minimum and maximum of the 1000 GHG budgets can be found, as well as the interquartile range (IQR) and the normalized interquartile range (NIQR), which is calculated as the IQR divided by the mean, multiplied with 100. In Fig. S8, the distribution of these bootstraps can be found.

Table S10: For each greenhouse gas, CO₂ (mg C m⁻² h⁻¹), CH₄ (μg C m⁻² h⁻¹) and N₂O (μg N m⁻² h⁻¹), the average, the minimum and maximum ($mean_{minimum}^{maximum}$) greenhouse gas budget of the 1000 bootstraps from the automated chamber measurements, together with the interquartile range (IQR) and the normalized interquartile range (NIQR, %) for each scenario.

	CO ₂	CH ₄	N ₂ O
Scenario a	176.0 ¹⁹² ₁₅₉	-44.2 ² ₋₅₉	40.0 ⁶² ₂₉
	IQR = 7.2 NIQR= 0.04	IQR = 8.5 NIQR= 0.19	IQR = 5.5 NIQR= 0.13
Scenario b	176.2 ¹⁸⁵ ₁₆₉	-45.2 ⁻³⁴ ₋₅₄	39.3 ⁴⁷ ₃₃
	IQR = 3.5 NIQR= 0.02	IQR = 4.1 NIQR= 0.09	IQR = 2.7 NIQR= 0.07
Scenario c	175.9 ¹⁷⁹ ₁₇₃	-44.7 ⁻⁴¹ ₋₄₈	40.3 ⁴⁴ ₃₈
	IQR = 1.3 NIQR= 0.01	IQR = 1.3 NIQR= 0.03	IQR = 1.1 NIQR= 0.03

Detection limit

Precision (1σ) of the analysers used in the set-up

CO₂ Measurements

3.5 ppm at 400 ppm with 1 second averaging

CH₄ Measurements

0.60 ppb at 2 ppm with 1 second averaging

N₂O Measurements

0.40 ppb at 330 ppb with 1 second averaging

Calculating the detection limit for the automated chambers by using 2 times the standard deviation divided by the closure time of 15 minutes as dq/dt in equation 1 from the article, results in a detection limit for CO₂ equal to 2.0 mg C m⁻² h⁻¹, for CH₄ equal to 0.3 μg C m⁻² h⁻¹ and for N₂O equal to 0.5 μg N m⁻² h⁻¹.

Calculating the detection limit for the fast box chambers by using 2 times the standard deviation divided by the closure time of 2 minutes as dq/dt in equation 1 from the article, results in a detection limit for CO₂ equal to 15.5 mg C m⁻² h⁻¹, for CH₄ equal to 2.6 μg C m⁻² h⁻¹ and for N₂O equal to 1.6 μg N m⁻² h⁻¹.